

Applying Parametric Analysis in Enhancing Performance for Double-Layer Scissor Lifts

Anh-Tuan Dang – Dang-Viet Nguyen – Dinh-Ngoc Nguyen*
Thai Nguyen University of Technology, Vietnam

This study presents a calculation procedure of applying the statistical method in determining design parameters for double-layer scissor lifts to improve their operation (e.g., lifting height, loading, stability). By parameterizing the mounting orientation of cylinders, the working of the mechanism is summarized as functions and evaluated. To verify the accuracy of obtained equations, a 2D model of the mechanism was constructed and simulated using Working Model software. The results obtained from the simulation indicate that by adjusting the mounting positions of cylinders, the platform's position and reactions on the device can be determined, enabling improvement of the system's performance. The results obtained from the study show the practical significance of applying parametric methods to the calculating process and optimizing the structure of multiple-layer scissor lifts.

Keywords: double-layer scissor lift, cylinder's orientation, kinematic analysis, parametric method

Highlights

- Applying parametric analysis for a distinctive model of a double-layer scissor lift to obtain the reactions of each joint in the whole mechanism.
- The proposed method can assist the calculation process without the need to construct 3D models for complex simulations.
- Based on the acquired reactions and position information, the structure of the system can be further optimized, reducing the production cost and the calculation time.
- From the initial design parameters, hydraulic cylinders can be easily selected to meet the designer's requirements.

0 INTRODUCTION

Scissor lifts are popular aerial platform lifts that use a scissor-shaped mechanism to lift objects or people over short distances in height. Although the first mechanism was used in Sweden in the early 1900s, it was not until the 1970s that scissor lifts gained popularity as commonly manufactured lifting structures. To select the appropriate lift for the job, lifting height, and loading are factors to be considered when choosing the equipment.

Based on the above requirements, several studies have been conducted on devices to test their functional ability. Solmazıyıt et al. [1] proposed the construction of and successfully manufactured a scissor lift device that enables lifting loads of up to 25 tons. Pan et al. [2] conducted a falling arrest test on a multi-layer scissor lift to check the structural stability, thereby ensuring tip-over safety for the system during the dropping process. Another study by Dong et al. [3] on an actual model also shows that the tip-over potential of the scissor lift system depends on the cylinder's speed. The study also indicates that the system's stability reduces when connecting joints are severely worn, or the structure is damaged.

In addition to manufacturing and testing on real devices, other studies also focus on theoretical models to evaluate the performance of lifting

systems to select the optimized layouts. Spackman [4] applied mathematical techniques to analyse the mechanism of n-layer scissor lifts. The study not only analysed the reactions in the scissor members but also presented some design issues related to actuator placement, member strength, and rigidity. Kosucki et al. [5] suggested using a volumetric controller to regulate the speed of the cylinders. With significant advantages such as a simple structure and low cost, the paper presents the possibility of extending the use of volumetric control to operate low-power driving systems. Karagülle et al. [6] employed finite element analysis (FEA) on a 3D model created in Solidworks to ascertain the internal loads acting on each component of a single-layer system. Dang et al. [7] proposed using the parametric method to model single-layer scissor lifts and construct mathematical equations to determine cylinder loads and reactions at the joints. Using the same approach, Todorović et al. [8] applied Harris Hawks optimization (HHO) to reduce mass in the mechanism frames. By solving static equations for a single-layer structure, Čuchor et al. [9] suggested an accurate method for selecting a hydraulic cylinder capable of lifting loads up to 3.5 tons.

These studies demonstrate the significant influence of the cylinder on the operation of the lifts. It can be observed that for 3D models

constructed using graphic software, the calculation process is only performed for limited positions, thus making it difficult to evaluate the overall impacts of the cylinder's operation. In contrast, employing mathematical equations as a solving approach can greatly reduce the calculation and testing time, providing a more efficient method.

In this study, a specific structure of a double-layer scissor lift consisting of two cylinders is selected for analysis (Fig. 1). By determining the mathematical relationship between the movements of the cylinders and the platform, designers can choose the suitable dimensional arrangement for the cylinders that is beneficial for the required lifting.

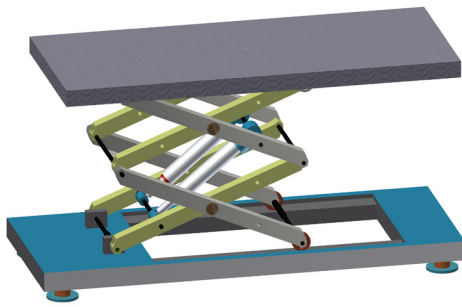


Fig. 1. Structure of the studied system

1 KINETIC ANALYSIS

From the 3D model of the system, a 2D model is represented, as shown in Fig. 2. The design problem can be described as follows: for a double-layer scissor mechanism with a fixed frame length a , designers must arrange two given hydraulic cylinders to utilize the maximum potential of the structure. Assuming the cylinders operate between the zero-stroke ($l_{Cyl.min}$) and full-stroke positions ($l_{Cyl.max}$) with a maximum thrust force F_{Cyl} , and the platform has a raising requirement of Δh .

The problem then becomes one of determining the mounting position of joints P and Q in the two connected frames (AF and FC) while ensuring the stability of the lift and limiting the loading on the cylinders. Analysis of the lift construction shows that when the cylinder operates (the distance between P and Q changes), platform 5 moves to the corresponding height h . Although the length of the frames (a) and the arrangement dimensions (FQ, FP) of the cylinder are fixed, the stability of the mechanism is altered (angles γ at joints between frames E and F, and the distance l between supports A and B). Since there are too many parameter dimensions involved in the operation,

designers may have difficulty choosing the correct layout to represent the movement of the platform.

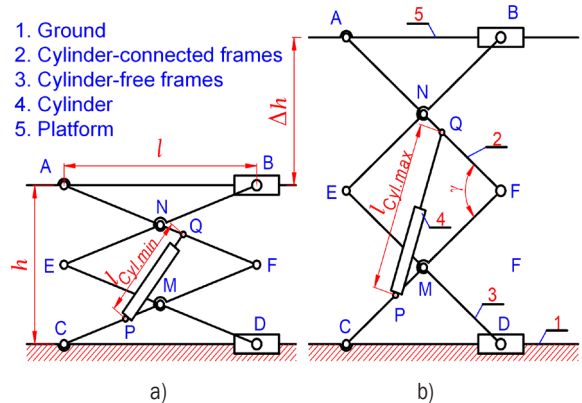


Fig. 2. Schematic diagram of the mechanism in: a) lowest position, and b) highest position

Assign parameters for assembling dimensions $QF = \beta_1 \cdot a$, $PF = \beta_2 \cdot a$, and $PQ = \lambda \cdot a$ (with $0 < \beta_1, \beta_2 < 1$, $\lambda_{max} > \lambda > \lambda_{min} > 0$ is the length ratio of the cylinder compared to one frame); the system is parameterized as shown in Fig. 3.

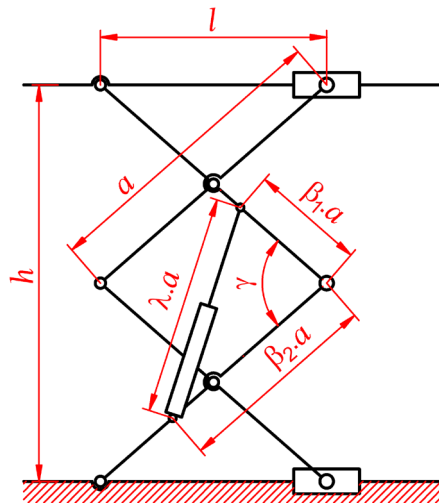


Fig. 3. Parameterizing the device in Fig. 2

When cylinder extends, platform height h can be calculated using the following equation:

$$h = 2a \sin \frac{\gamma}{2} = 2a \sqrt{\frac{1 - \cos \gamma}{2}} \quad (1)$$

The angle γ between frames is determined based on the relationship of the triangle MPQ:

$$\cos \gamma = \frac{\beta_1^2 + \beta_2^2 - \lambda^2}{2\beta_1\beta_2} \quad (2)$$

Substitute Eq. (2) into Eq. (1); the height of the platform can be determined by the layout dimensions of the structure:

$$h = a \sqrt{\frac{\lambda^2 - (\beta_1 - \beta_2)^2}{\beta_1 \beta_2}}. \quad (3)$$

The lifting efficiency of the system can be evaluated by the lifting ratio, which is determined by the lifting height of the platform when the cylinder extends its length from zero-stroke to full-stroke:

$$k_h = \frac{h_{\max} - h_{\min}}{a} = f(\lambda_{\max}, \lambda_{\min}, \beta_1, \beta_2). \quad (4)$$

It should be noted that when the platform is raised, γ between the frames increases and the loading distance between supports l decreases, which is also a factor affecting the stability of lift. This distance can be calculated using the equation:

$$l = a \cos \frac{\gamma}{2} = a \sqrt{\frac{(\beta_1 + \beta_2)^2 - \lambda^2}{4\beta_1 \beta_2}}. \quad (5)$$

2 FORCE ANALYSIS

As described in the modelling step, due to the symmetry of the 3D structure, it is possible to investigate the reactions on the lift by analysing force on one side of the system. If the loading is $2P'$, the reactions at the bearings and cylinders in Fig. 2 can be correspondingly determined in terms of $P_G = (P' + W_p)/2$ (where W_p represents the weight of the platform, and G is the centroid of the total load P_G). In practice, the load on the system, specifically the lifting load P_G on the platform, may continuously change during the operation of the device. This occurs when workers walk on the platform to perform repair and maintenance tasks while the lift is still in motion. This situation not only exerts forces on joints but also causes deformation of the component frames, including bending, compression, or tensile stresses. Since these frames can be designed with rigid and sustainable materials, the impact of forces on them can be ignored, allowing the problem to be focused on revolution joints where bearings are assembled.

In the scope of this study, this paper is only concerned with analysing the static influence of forces on the structure (it considers that the load P_G is fixed on the platform during the movement of the cylinder, and the frame weight W of each frame is at its centre). This means that the distance between point G and support A is constant when lifting persons or objects from height h to h' (see Fig. 4). However, since the

support distance l changes during the operation of cylinders, the magnitude of loads acting on joints A and B also changes, influencing the balance of the device and reactions on joints.

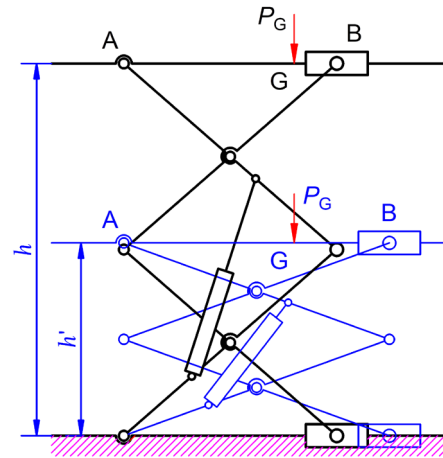


Fig. 4. Location of load P_G when the platform raises from the lowest to the highest position

Assuming that the platform is raised slowly enough that the effect of acceleration can be ignored. Given the load on the system and the cylinder's weights are much smaller than the weight of the frames (W), the calculation of reactions on the structure can be outlined in the following steps:

First, the scissor structure is separated from moving platform 5 and ground platform 1 (see Fig. 5). Based on this figure, the reactions at supports A and B can be determined using moment equilibrium equations:

$$P_B = P'_B = \frac{P_G l_G}{l}, \quad (6)$$

$$P_A = P'_A = P_G - P_B = P_G - \frac{P_G l_G}{l}. \quad (7)$$

Similarly, the reactions at supports C and D can be calculated as:

$$P_C = P'_C = \frac{P_G l_G + 4W \frac{l}{2}}{l} = \frac{P_G l_G}{l} + 2W. \quad (8)$$

$$P_D = P'_D = P_G - \frac{P_G l_G}{l} + 2W. \quad (9)$$

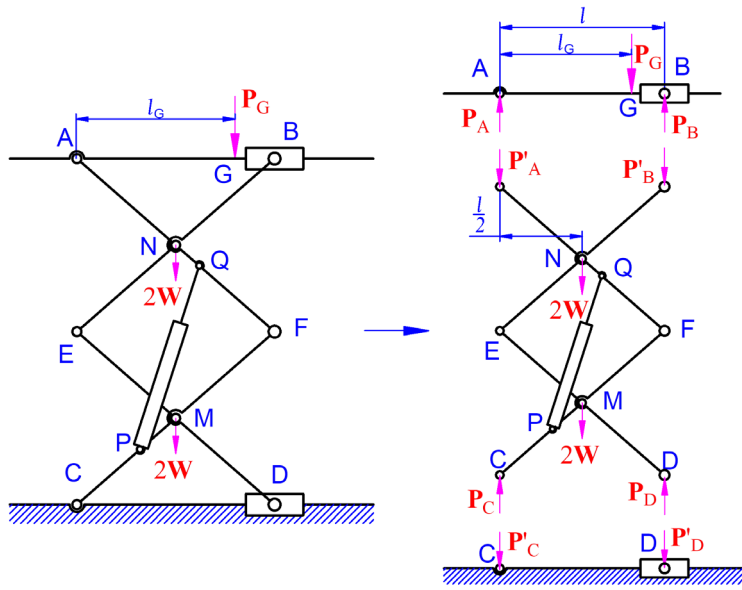


Fig. 5. Separating component frames to determine reactions in the mechanism

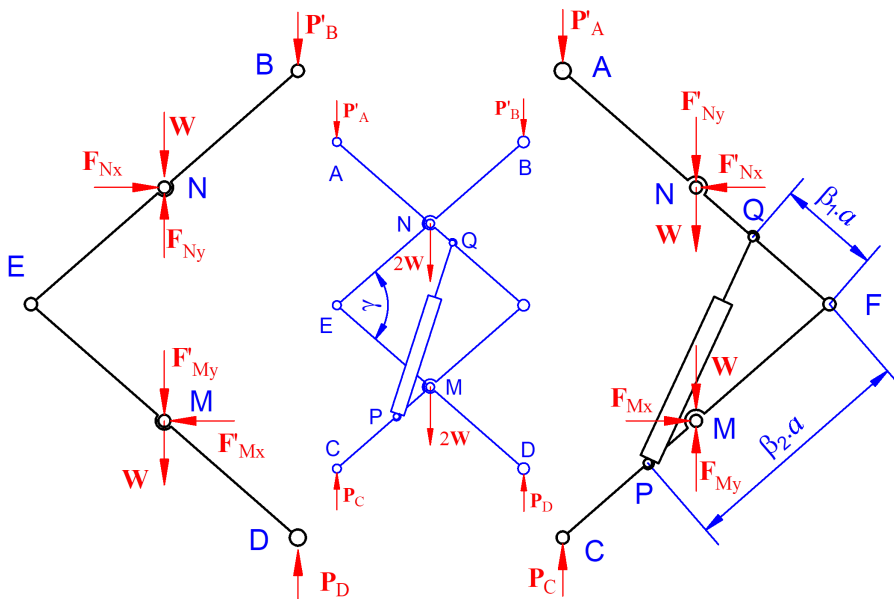


Fig. 6. Release the connection at joints M and N

Second, release the connection at joints M and N, and separate these reactions into directional components F_x and F_y . (see Fig. 6):

Balancing the moment in DEB frame:

$$\sum M_E = 0, \rightarrow$$

$$(P_D - P'_B) a \cos \frac{\gamma}{2} - (F_{Mx} + F_{Nx}) \frac{a}{2} \sin \frac{\gamma}{2}$$

$$+ (W_{Ny} - 2W - F_{My}) \frac{a}{2} \cos \frac{\gamma}{2} = 0. \quad (10)$$

Third, continuing to release connections at E, F, and apply the moment equilibrium equation at point E for BE frame (see Fig.7);

$$\sum M_E = (F_{Ny} - W) \frac{a}{2} \cos \frac{\gamma}{2}$$

$$- P'_B a \cos \frac{\gamma}{2} - F_{Nx} \frac{a}{2} \sin \frac{\gamma}{2} = 0. \quad (11)$$

Draw F_{Nx} and F_{Mx} from Eq. (10):

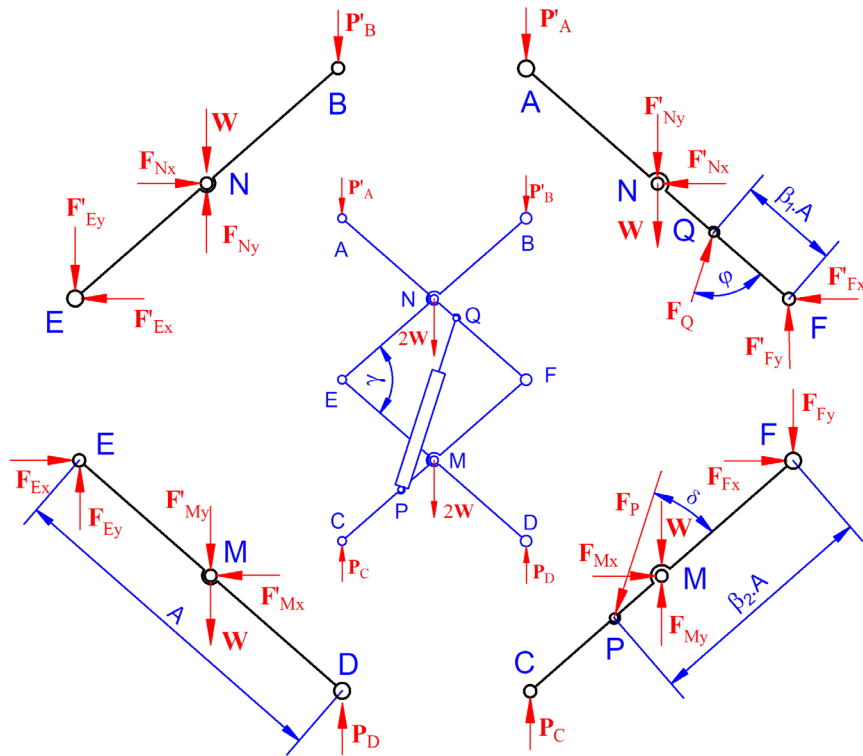


Fig. 7. Release the connection at joints E and F

$$F_{Nx} = F_{Mx} = \frac{W}{\tan \frac{\gamma}{2}} \quad (12)$$

Draw F_{Ny} from Eq. (12):

$$F_{Ny} = 2P'_B + 2W = 2 \left(\frac{P_G l_G}{l} + W \right) \quad (13)$$

Apply the moment equilibrium equation for AF frame:

$$\sum M_F = P'_A a \cos \frac{\gamma}{2} + (F_{Ny} + W) \frac{a}{2} \cos \frac{\gamma}{2} + F_{Nx} \frac{a}{2} \sin \frac{\gamma}{2} - F_Q \beta_1 a \sin \varphi = 0 \quad (14)$$

Substitute Eqs. (7), (12) and (13) into Eq. (14) and draw the cylinder's thrust force F_Q :

$$F_Q = \frac{(P_G + 2W)\lambda}{2\beta_1\beta_2 \sin \frac{\gamma}{2}} = \frac{(P_G + 2W)\lambda}{\sqrt{\beta_1\beta_2 [\lambda^2 - (\beta_1 - \beta_2)^2]}} \quad (15)$$

It can be observed that the coefficient l_G in Eq. (15) has been omitted, implying that the position of loading P_G does not impact the magnitude of thrust force in cylinders. However, as this parameter remains

present in the reaction at other joints, their magnitudes will vary and influence the stability of the system. By applying the equilibrium equation for frame AF, directional reactions at joint F can be computed as:

$$F_{Fx} = F_Q \cos \left(\frac{\gamma}{2} + \varphi \right) - F_{Nx} \quad (16)$$

$$F_{Fy} = -F_Q \cdot \sin \left(\varphi + \frac{\gamma}{2} \right) + F_{My} + P'_A + W \quad (17)$$

Substitute β_1, β_2 and λ into these equations:

$$F_{Fx} = \left[\frac{(P_G + 2W)(\beta_2 - \beta_1)}{2\beta_1\beta_2} - W \right] \sqrt{\frac{(\beta_1 + \beta_2)^2 - \lambda^2}{\lambda^2 - (\beta_1 - \beta_2)^2}} \quad (18)$$

$$F_{Fy} = P_G + \frac{P_G l_G}{a} \sqrt{\frac{4\beta_1\beta_2}{(\beta_1 + \beta_2)^2 - \lambda^2}} + 3W - \frac{(P_G + 2W)(\beta_1 + \beta_2)}{2\beta_1\beta_2} \quad (19)$$

The total reactions in the remaining joints can be determined by combining their directional components:

$$F_E = \sqrt{F_{Ex}^2 + F_{Ey}^2} \quad (20)$$

3 RESULTS

$$F_F = \sqrt{F_{Fx}^2 + F_{Fy}^2}, \quad (21)$$

$$F_M = F_N = \sqrt{F_{Nx}^2 + F_{Ny}^2}. \quad (22)$$

To validate the accuracy of the calculation method, five 2D physical models were created using Working

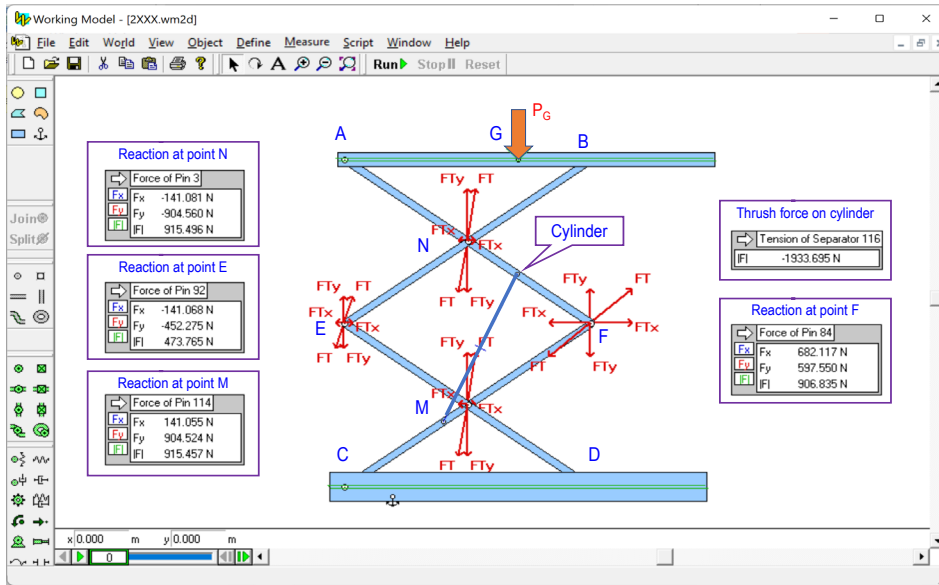


Fig. 8. Export reactions at joints using Working Model

Table 1. Compare result of forces between calculation method and 2D model simulation

$a = 1 \text{ m}; W = 75 \text{ N}; P_G = 5000 \text{ N}$		$l_G = 1 \text{ m}$			$l_G = 5 \text{ m}$		
		F_1 [N]	F_2 [N]	D [%]	F_1 [N]	F_2 [N]	D [%]
$\beta_1 = 0.20$ $\beta_2 = 0.65$ $l = 0.46$	FCyl	68,865.00	68,876.76	0.02	68,866.50	68,876.76	0.01
	FM	807.30	807.18	(0.01	2,657.36	2,657.27	0.00
	FE	67,138.51	67,150.27	0.02	66,835.78	6,846.14	0.02
	FF	1,288.87	1,287.93	0.07	5,224.77	5,224.64	0.00
$\beta_1 = 0.20$ $\beta_2 = 0.65$ $l = 0.74$	FCyl	17,991.60	17,992.64	0.01	17,990.90	17,992.64	0.01
	FM	938.33	938.66	0.04	4,385.43	4,386.01	0.01
	FE	12,454.58	12,455.55	0.01	9,637.26	9,638.13	0.01
	FF	1,874.53	1,875.04	0.03	8,770.51	8,771.54	0.01
$\beta_1 = 0.20$ $\beta_2 = 0.80$ $l = 0.62$	FCyl	50,998.50	51,102.72	0.20	51,006.00	51,102.72	0.19
	FM	693.59	695.64	0.30	2,647.89	2,650.97	0.12
	FE	49,127.06	49,227.89	0.20	48,696.98	48,839.48	0.29
	FF	1,225.13	1,228.80	0.30	5,257.09	5,261.63	0.09
$\beta_1 = 0.10$ $\beta_2 = 0.30$ $l = 0.22$	FCyl	71,199.00	71,372.29	0.24	71,226.80	71,372.29	0.20
	FM	652.18	653.41	0.19	2,678.20	2,681.35	0.12
	FE	68,427.42	68,545.39	0.17	67,549.09	67,706.62	0.23
	FF	1,215.76	1,218.03	0.19	5,334.71	5,341.76	0.13
$\beta_1 = 0.25$ $\beta_2 = 0.50$ $l = 0.30$	FCyl	26,339.80	26,351.61	0.04	26,339.80	26,351.61	0.04
	FM	665.36	666.31	0.14	2,664.44	2,664.92	0.02
	FE	23,158.51	23,169.49	0.05	22,373.90	22,385.29	0.05
	FF	1,217.95	1,219.00	0.09	5,301.81	5,302.57	0.01

with F_1 is reaction measured from Working Model;

F_2 is reaction obtained by calculation; and $\Delta = \left| \frac{F_1 - F_2}{F_2} \right| \times 100 [\%]$ is the difference between the two methods.

Model software to measure the reactions at the joints (refer to Fig. 8). The obtained results from this step are then compared with the results calculated using equations, as presented in Table 1.

The first two models represent the results of the same structure with cylinder lengths of 0.46 m and 0.74 m, respectively. The remaining models depict structures with random cylinder orientations. The differences of less than 0.3 %, demonstrate the accuracy of the calculation model in determining the reactions in the mechanism. This indicates that we can accurately determine the design parameters without the need to construct or simulate the system in 3D virtual models, which can be time-consuming.

For detailed analyses, constraints such as the range of frame angular movement are applied ($\gamma_{\min} = 10^\circ$ and $\gamma_{\max} = 120^\circ$), the operational length of

the cylinder (50 mm for zero-stroke and 80 mm for full-stroke, corresponding to $\lambda_{\min} = 0.5$ and $\lambda_{\max} = 0.8$ for the given model with $a = 1$ m), and the maximum thrust force $F_{Cyl} = 16$ kN. Based on this information, two graphs of lifting ratio k_h and the maximum loading for the cylinder at zero-stroke (lowest position) are constructed, as presented in Fig. 9.

The graph also indicates that to achieve the highest efficiency for the cylinder (maximum lifting ratio), the cylinder orientation must be selected as $\beta_1 = 0.31$ and $\beta_2 = 0.65$; Additionally, the loads in the other joints of this system can also be calculated, as shown in Fig. 10.

Eq. (3) shows that the position of the platform is determined by the displacement of the cylinder l_{Cyl} and the arrangement coefficients β_1, β_2 . This implies that

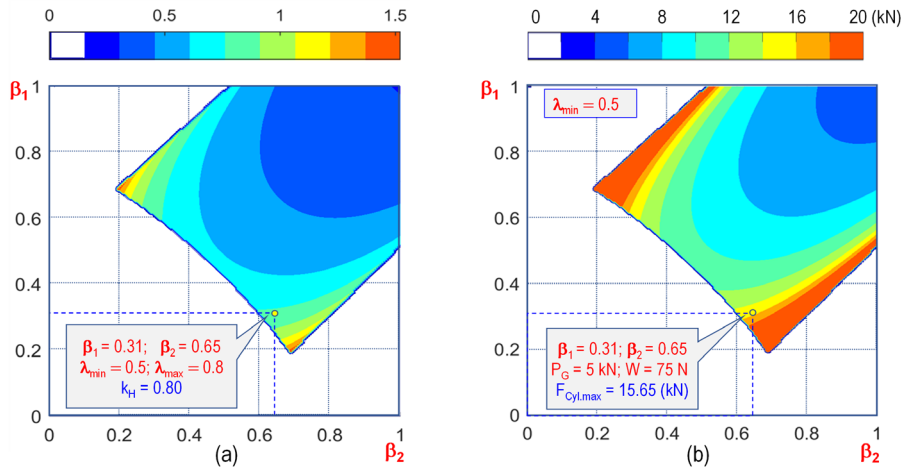


Fig. 9. Graphs constructed from the given data (β_1, β_2); a) lifting ratio k_h , and b) maximum thrust force F_{Cyl}

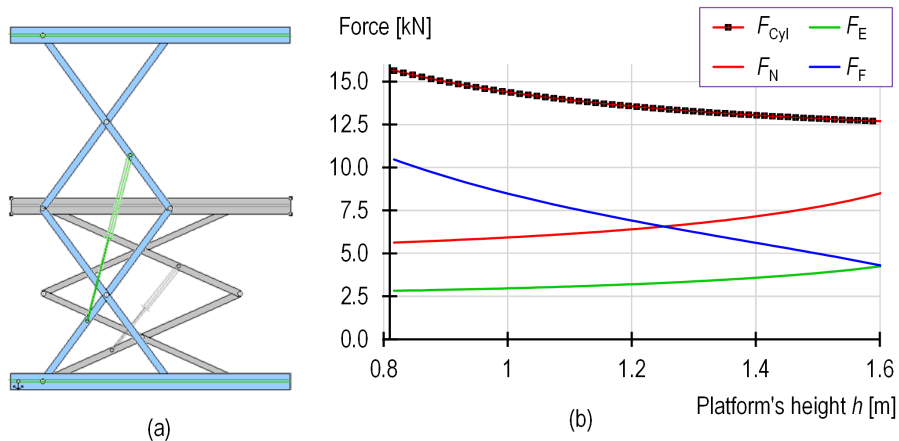


Fig. 10. Structure of the new system: a) highest and lowest positions of the lift; and b) reactions on joints corresponding the movement of platform

the lifting velocity of the platform can be determined by taking the derivative of Eq. (3):

$$\dot{h} = \frac{A\lambda\dot{\lambda}}{\sqrt{\beta_1\beta_2[\lambda^2 - (\beta_1 - \beta_2)^2]}} \quad (23)$$

where $\dot{\lambda}$ is the extend rate of the cylinder.

The equation also indicates that by controlling the oil pump system, designers have the ability to modify the system's operation, particularly the movement of the platform. This feature can be achieved by using a time-control unit for the pumping system, allowing for complex platform movements. such as acquiring the complex movement of the platform by using a time-control unit for the pumping system. Fig. 11 illustrates the platform movement for a specific system selected from Fig. 10, in which the cylinder moves at different constant speeds of 1 m/s, 2 m/s, and 5 m/s. This corresponds to operation times for cylinder extension from zero stroke to full stroke length of 60 s, 150 s, and 300 s, respectively.

The results from Fig. 11 show that when the cylinder extend or raises the platform at a slower rate, there is a smaller difference in velocity during the movement. Conversely, faster movement of the cylinder leads to system instability, as varying velocity not only causes vibration but also creates acceleration and inertia forces.

Another application of the parametric method is selecting the appropriate cylinder in case the position of the cylinder has been given. For example, if the dimensions for the cylinders' arrangement are $\beta_1 = 0.3$ and $\beta_2 = 0.6$, the structure of the cylinder (length, stroke and force) can be calculated and summarized as shown in Fig. 12.

According to the requirement for structural stability, the angle γ between frames should be adjusted between 10 degrees and 120 degrees, meaning the cylinder length should be selected between 0.31 meters and 0.8 meters, according to Eq. (2).

Suppose the platform is required to be raised 0.5 meters. In that case, we can either select the cylinder with a 32 cm initial length and 12 cm stroke

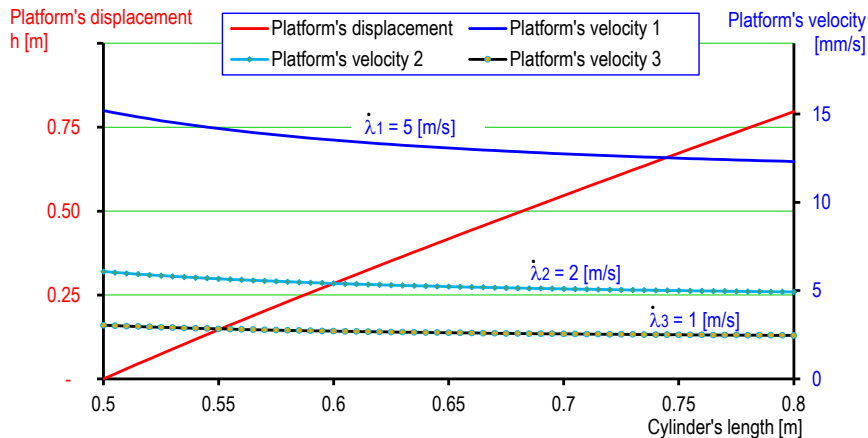


Fig. 11. Movement of platform for selected structure with cylinder moving extends with different speeds

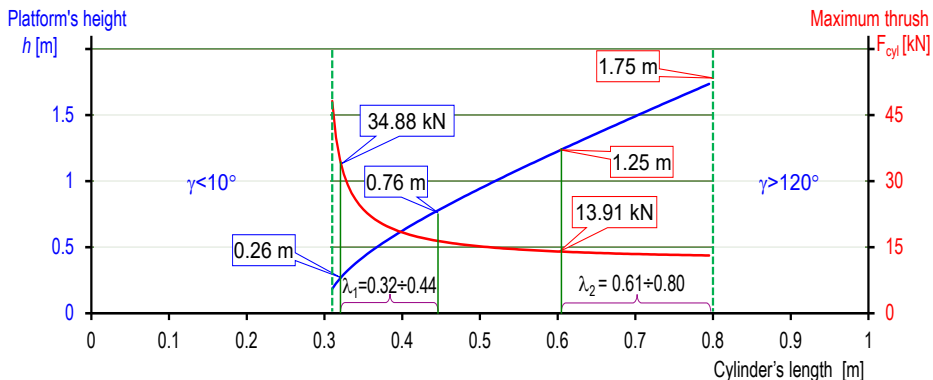


Fig. 12. Data of cylinder corresponding to the raising height and loading requirement ($a = 1$ m; $\beta_1 = 0,3$; $\beta_2 = 0,6$; $P_G = 5$ kN; $W = 75$ N)

(corresponding to $h_{\min} = 0.26$ m and $h_{\max} = 0.76$ m) with a maximum capacity of $P_{\max} = 34.88$ kN or select another one with a 61 cm initial length and 19 cm stroke ($h_{\min} = 1.25$ m, and $h_{\max} = 1.75$ m) with a maximum capacity $P_{\max} = 13.91$ kN (having a longer stroke but a smaller thrust force requirement).

4 CONCLUSIONS

This study analyses the applicability of the parametric method in designing double-layer scissor lifts. The conclusions drawn from the study are presented as follows:

- By using simple dimensional parameters, it is possible to determine the important information of double-layer scissor lifts, such as the platform's height, cylinder's thrust force, and loading in revolution joints. This enables easy component selection without the need for complex 3D modelling or experimental tests.
- The parametric method allows for efficient selection of the appropriate cylinder based on design parameters and the given requirements.
- By analysing the reactions and position of the lift, it is possible to optimize the structure of the system, leading to cost reduction and shorter calculation time.

5 ACKNOWLEDGEMENTS

The authors wish to thank Thai Nguyen University of Technology for supporting this work.

6 REFERENCES

- [1] Solmazıyıt, İ., Bařkurt, R.C., Ovalı, İ., Tan, E. (2022). Design and prototype production of scissor lift platform 25 tons capacity. *The European Journal of Research and Development*, vol. 2, no. 4, p. 326-337, DOI:10.56038/ejrnd.v2i4.177.
- [2] Pan, C.S., Powers, J.R., Hartsell, J.J., Harris, J.R., Wimer, B.M., Dong, R.G., Wu, J.Z. (2012). Assessment of fall-arrest systems for scissor lift operators: computer modeling and manikin drop testing. *Human Factors*, vol. 54, no. 3, p. 358-372, DOI:10.1177/0018720811425024.
- [3] Dong, R.G., Pan, C.S., Hartsell, J.J., Welcome, D.E., Lutz, T., Brumfield, A., Harris, J.R., Wu, J.Z., Wimer, B., Mucino, V., Means, K. (2012). An investigation on the dynamic stability of scissor lift. *Open Journal of Safety Science and Technology*, vol. 2, no. 1, p. 8-15, DOI:10.4236/ojsst.2012.21002.
- [4] Spackman, H. M. (1989). Mathematical Analysis of Scissor Lifts. Naval Ocean Systems Center San Diego Ca.
- [5] Kosucki, A., Stawiński, Ł., Morawiec, A., Goszczak, J. (2021). Electro-hydraulic drive of the variable ratio lifting device under active load. *Strojniški vestnik - Journal of Mechanical Engineering*, vol. 67, no. 11, p. 599-610, DOI:10.5545/sv-jme.2021.7320.
- [6] Karagülle, H., Akdağ, M., Bülbül, İ. (2022). Design automation of a two scissors lift. *The European Journal of Research and Development*, vol. 2, no. 4, p. 178-191, DOI:10.56038/ejrnd.v2i4.192.
- [7] Dang, A.T., Nguyen, D.N., Nguyen, D.H. (2021). A study of scissor lifts using parameter design. Sattler, KU., Nguyen, D.C., Vu, N.P., Long, B.T., Puta, H. (Eds) *Advances in Engineering Research and Application. Lecture Notes in Networks and Systems*, vol. 178, Springer, Cham, p. 75-85, DOI:10.1007/978-3-030-64719-3_10.
- [8] Todorović, M., Zdravković, N. B., Savković, M., Marković, G., Pavlović, G. (2021). Optimization of scissor mechanism lifting platform members using HHO method. *The 8th International Conference, Transport And Logistics*, p. 91-96.
- [9] Čuĥor, M., Kuĥera, L., Dzimko, M. (2021). Engineering design of lifting device weighing up to 3.5 tons. *Transportation Research Procedia*, vol. 55, p. 621-628, DOI:10.1016/j.trpro.2021.07.095.